

By acceptance of this article, the publisher or recipient acknowledges the U.S. Government's right to retain a nonexclusive, royalty-free license in and to any copyright covering this article.

NEUTRAL PUMPING RATES FOR A NEXT STEP TOKAMAK IGNITION DEVICE*

J. D. Galambos, Y-K. M. Peng, FEDC/Cek Ridge National Laboratory
P. O. Box Y FEDC Building
Oak Ridge, TN 37831
(615) 576-5449

D. Heifetz, Princeton Plasma Physics Laboratory

ABSTRACT

Neutral pumping rates are calculated for pump-limiter and divertor options of a next step tokamak ignition device using a method that accounts for the coupled effects of neutral transport and plasma transport. For both pump limiters and divertors the plasma flow into the channel surrounding the neutralizer plate is greatly reduced by the neutral recycling. The fraction of this flow that is pumped can be large (>50%) but in general is dependent on the particular geometry and plasma conditions. It is estimated that pumping speeds $\geq 10^5$ L/s are adequate for the exhaust requirements in the pump-limiter and the divertor cases.

I. INTRODUCTION

Studies on tokamak scrape-off (S.O.) characteristics have been primarily directed toward identifying radial profiles of the plasma parameters for the purpose of limiter (or divertor plate) design. Most of these studies¹⁻⁵ rely on relatively simple models for plasma transport along field lines, although more sophisticated models⁶⁻¹⁰ have been used and have identified a regime of operation characterized by low temperatures and high densities at the neutralizer plate. Less attention has been given to the issue of neutral pumping. Most previous neutral pumping predictions^{1-3, 11, 12} are derived from models using simplified treatments of the plasma transport. However, the more sophisticated models show that there is an important interaction between the plasma and neutrals near the divertor plate (or pump-limiter) that has a strong effect on the plasma transport along the field lines (see Refs. 6-9, 13, 14). This study investigates neutral pumping rates

* Research sponsored by the Office of Fusion Energy, U.S. Department of Energy, under Contract No. DE-AC05-84OR21400 with Martin Marietta Energy Systems, Incorporated.

DISCLAIMER

This report was prepared as an account of work sponsored by an agency of the United States Government. Neither the United States Government nor any agency thereof, nor any of their employees, makes any warranty, express or implied, or assumes any legal liability or responsibility for the accuracy, completeness, or usefulness of any information, apparatus, product, or process disclosed, or represents that its use would not infringe privately owned rights. Reference herein to any specific commercial product, process, or service by trade name, trademark, manufacturer, or otherwise does not necessarily constitute or imply its endorsement, recommendation, or favoring by the United States Government or any agency thereof. The views and opinions of authors expressed herein are not necessarily state or reflect those of the United States Government or any agency thereof.

for a next-step-type ignition device using a model that couples the plasma and neutral transport effects. The method used here is outlined in the following section. (Ref. 15 contains a detailed description of the model.) Section III presents results for the pump-limiter and divertor.

II. METHOD

The method used to calculate the neutral pumping rates involves iteration between several models. This process begins by calculating the radial plasma profiles in the S.O. The model used for this profile calculation differs from previously used one-dimensional (1-D) radial transport S.O. models in the treatment of the terms that account for the losses of particles and energy along the field lines. A two-point model^{13, 14} is used here to evaluate the axial loss terms. This model is analytic in nature, accounts for the effects of neutral recycling on plasma flow rates along the field, and includes heat conduction along the field lines. It is necessary to provide the two-point model with a guess for the neutral recycling that occurs at the neutralizer plate. Output from this model includes the S.O. width and the radially averaged density and temperatures. These values are used as input to the ZEPHYR⁸ code that models plasma transport along the field lines. An analytically based neutral transport model that accounts for the pumping effects¹¹ is used in conjunction with ZEPHYR. The neutral recycling found in this latter step is checked against that assumed in the two-point model, and the entire loop is redone if the recycling values do not coincide. Also, the simple neutral transport model used with ZEPHYR is benchmarked with the Monte Carlo neutral transport code DEGAS.¹⁵

Each of the components in the previously described iteration loop is inadequate by itself to model the entire process of plasma

MASTER

transport in the S.O. along and across field lines, and to model the coupled effects from neutral transport. Each component relies on input and checks from other components. By separating the modeling process in this manner, it is possible to obtain solutions without excessive numerical effort while retaining the salient features of the individual models. The following is a description of the different components involved in the model.

In the radial profile model, the S.O. field lines are divided into two axial regions along the field lines: (1) the length L_1 alongside the main plasma in which no neutral recycling is accounted for and (2) the length L_2 in the divertor region (or beneath the limiter) in which all the recycling of neutrals formed on the neutralizer plate is assumed to occur. (Calculations presented in Ref. 15 indicate this is a good assumption.) The common point of the two regions is designated as the throat (t) entrance. In the first region, it is assumed that the temperature (T) and density (n) are constant along the field line. (Full 1-D calculations along the field^{6,8} show that important n and T gradients do appear in region 2.) The values of n and T in region 1 are used as input conditions at the throat for a two-point method^{13,14} that analyzes the transport along the field between the throat and neutralizer plate (p). Boundary conditions at the sheath adjacent to the neutralizer plate used in the two-point model are that the flow Mach number is 1, and the heat flux is $8nTV$. Also, the neutral recycling coefficient is defined as

$$R = 1 - (nV)_c / (nV)_p,$$

where V is the plasma flow speed along the field lines and is calculated for each radial position. Output from the two-point model includes the heat flux and particle flow speed at the throat. These quantities are used to find the exponential decay lengths (in the radial direction) for plasma density and temperature following the prescription described in Ref. 1. The exponential falloff is approximately correct in some small radial increment in which the loss rates along the field lines and the cross field particle (energy) transport coefficient $D(\chi)$ do not change much. Radial profiles over the entire S.O. are found as follows: start with a specified temperature and density at the main plasma S.O. interface; use the two-point method to find the axial loss terms; find "local" exponential decay length; find temperature and density some small increment outwards; use two-point method to find the new axial loss rates, etc.

The primary tool used to investigate the plasma along S.O. field lines is the ZEPHYR code, developed at Culham. To include the effects of neutral recycling and the evaluation of neutral pumping rates, the neutral transport

model described in Ref. 11 has been coupled to the version of ZEPHYR used in this discussion. Detailed descriptions of ZEPHYR and the neutral transport model are provided in Refs. 8 and 11, respectively, and the coupling procedure is described in Ref. 15, so only a brief outline is presented.

The ZEPHYR code finds the steady-state plasma parameters between the watershed (or symmetry) point (point A in Fig. 1) and the neutralizer plate. ZEPHYR requires input values for the density, the ion and electron temperatures at the watershed (taken from the radial profile model), the flow Mach number at the plate (≈ 1.0 throughout this work), the ion and electron heat transfer coefficients across the sheath at the plate (≈ 4.0), and the neutral density profile. All cases assume a neutral density profile that decays exponentially with distance along the field line (away from the neutralizer plate). Output from ZEPHYR includes the neutral ionization rate.

The neutral transport model from Ref. 11 that is coupled to ZEPHYR is analytic in nature, which allows for a fast iteration procedure with the ZEPHYR code. The geometry used in the neutral transport model is shown in Fig. 1. The method used in this model involves finding the average probability that a neutral

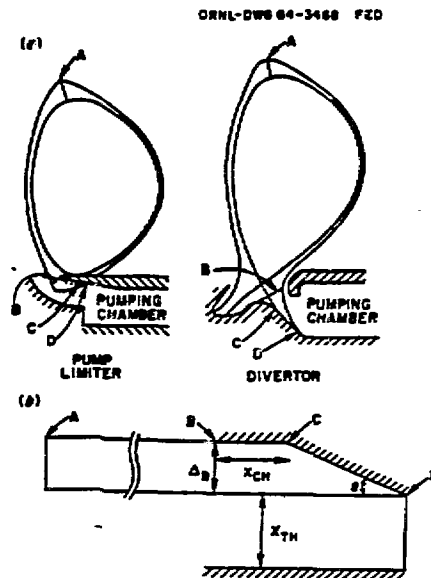


Fig. 1. (a) Schematic of actual scrape-off geometry. (b) Approximate geometry used in ZEPHYR and the simple neutral transport model.

produced on the plate can escape through the wedge-shaped plasma cross section. The net neutral flux leaving the scrape-off is determined, accounting for multiple reflections off the chamber walls and passes through the scrape-off plasma [see Eqs. (35)-(44) in Ref. 11]. The portion of this neutral flux that is pumped, f_p , is governed through a balance of the effective area of the pumps, and the surface area of the plasma in the divertor channel. The model also estimates the fraction of neutrals produced at the plate that escape the divertor region (towards the main plasma).

The simple neutral transport model used in conjunction with ZEPHYR is benchmarked with the 3-D Monte-Carlo neutral transport code DEGAS¹⁶ for both the divertor and pump-limiter cases. Remarkably good agreement between the two models for the recycling (i.e. ionizing) fraction was found which was $\geq 80\%$ for the cases examined here. The smaller fractions of escaping and pumped neutrals calculated by the two models differed by as much as 50%, however. The simple neutral transport model was calibrated so that it calculated escaping and pumping rates in good agreement with those from DEGAS for both the pump-limiter and divertor geometries. Details of this comparison are presented in Ref. 15.

The iteration procedure between ZEPHYR and the neutral transport model involves changing the magnitude of the neutral density profile assumed in ZEPHYR to satisfy the steady-state neutral particle balance:

$$\text{ionization rate} + \text{pumping rate} + \text{escape rate} = \text{production rate} \quad (1)$$

Provided with an initial guess for the neutral density profile in the plasma, ZEPHYR calculates the plasma conditions at the neutralizer plate. With the additional knowledge of the scrape-off width (from the radial profile model), the total neutral production rate can be determined and the fractions that are pumped and that escape are provided by the neutral transport model. The magnitude of the neutral density is adjusted so that the total sink rate of neutral particles [left-hand side of Eq. 1] balances the production rate.

III. RESULTS

The first step in the S.O. modeling technique involves using the radial profile model to find the average density and temperature in region 1 of the S.O. and the S.O. thickness. Figure 2 shows the temperature and density radial profiles in the region adjacent to the main plasma. This case is for a density of $5 \times 10^{13} \text{ cm}^{-3}$ and a temperature of 140 eV at the main plasma scrapeoff interface (edge) and uses $D = \chi = 10^4 \text{ cm}^2/\text{s}$ for the particle and energy transport coefficients. Also shown is

the assumed neutral recycling profile, R , which is determined from the ZEPHYR neutral transport analysis. As seen in Fig. 2, the recycling decreases to zero in the radial extent where $20 > T(\text{eV}) > 10$, since the ionization probability drops rapidly below 20 eV. Also for the pump-limiter, the recycling is assumed to be small on the front surface of the limiter blade ($r < 2.2 \text{ cm}$ in Fig. 2). (Sensitivity of the results to these assumptions on the shape of the recycling vs r is addressed later.)

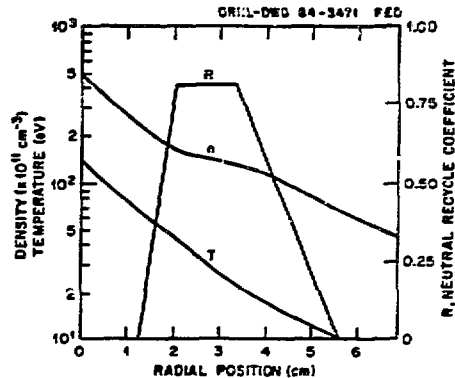


Fig. 2. Density n , temperature T , and neutral recycle coefficient R vs. radial distance from main plasma for a limiter case.

The distinguishing feature in Fig. 2 is the reduced rate of density falloff in the region of high neutral recycling, due to the reduction of the flow speed along the field lines. Also, it is evident that the temperature falloff is not reduced in this region because heat conduction allows energy transport along the field lines even though the particle flow rate in that direction is reduced. The integrated heat (Q) flux onto the limiter is 48 MW (including the outboard half of the scrape-off that is assumed to be the same as the inboard half modeled here). To arrive at a different integrated value for total heat flux, the starting values for n and/or T at the edge of the main plasma must be changed accordingly and the preceding process repeated.

The information displayed in Fig. 2 includes the thickness of the scrapeoff plasma that flows behind the limiter, Δ , and the average throat density \bar{n} and temperature \bar{T} of the plasma that flows behind the limiter. The thickness Δ is taken to be the radial distance from the leading edge to the point where the neutral recycling goes to zero. This information is used as input for the coupled ZEPHYR-neutral transport model calculation. Results for the plasma profiles along the field lines calculated with this model are shown in Fig. 3. The plasma density n , temperature T , and flow

speed V are relatively constant in the region adjacent to the main plasma [$4 \leq z$ (m) ≤ 20]. For this example, a pumping system with a pump speed (S_{eff}) of 2.2×10^5 L/s is modeled. The net plasma current entering the limiter shadow region for this case is 7.4×10^{21} s $^{-1}$, of which 4.7×10^{21} s $^{-1}$ (63%) are pumped as neutrals. Also, the neutral recycling in the divertor channel for these plasma conditions is 0.8, which is consistent with the assumed recycling in the preceding radial profile calculation.

Table 1 shows results for several other cases found using the procedure previously described. These cases investigate the effects on the calculated neutral pumping rates caused by variations in the assumed conditions at the main plasma-S.O. interface and by changes in the assumptions used in the model. Values provided by the radial profile model (Q , Δ , \bar{n} , \bar{T}) are indicated in the left-hand columns.

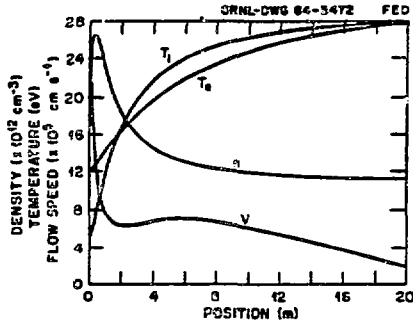


Fig. 3. Density (n), flow speed (V) temperature (ion-i, electron-e) vs. distance along field line for a limiter case.

Here $\Delta_{\text{S.O.}}$ is the total S.O. width, including the portion incident on the front surface of the limiter. Output from the coupled ZEPHYR-neutral model for the recycling value R , neutral pumping rate Γ_p , and the fraction of the plasma flow into the throat that is pumped f are shown in the right-hand columns. All cases in Table 1 use the same pump speed as the case described previously (case 1).

In comparing the neutral pumping rates in Table 1, the following scaling should be kept in mind. The neutral pumping rate is proportional to the total particle flow underneath the limiter (into the throat). For the pump-limiter case considered here, about one-half to two-thirds of this flow is pumped. The plasma flow under the limiter is

$$\Gamma_T \sim \Delta \times \bar{n}_t \times V_t, \quad (2)$$

where V_t is the plasma flow speed at the throat.

For conditions typical of the plasma considered here, the plasma flow speed at the throat is most strongly affected by the neutral recycling that occurs near the neutralizer plate, R . Increases in R tend to decrease the throat flow speed (see Ref. 13). Variations of the pumping rates shown in Table 1 are explained by variations in the three parameters on the right-hand side of Eq. (2) as discussed in the following paragraphs.

Increasing χ (case 2 compared to case 1) results in a wider S.O., which tends to increase the neutral recycling. The increased recycling slows the plasma flow rate into the throat, which overwhelms the effects of a larger Δ and results in a net decrease of the neutral pumping. Increasing D (case 3 vs. case 1) only slightly changes Δ , but in this case there are stronger gradients along the field line and a lower plate temperature (< 20 eV).

Table. 1. Results for coupled plasma-neutral transport modeling procedure for the limiter case.

Case	Radial Profile Model				Coupled ZEPHYR-neutral Model						
	n_{edge} (10^{13} cm $^{-3}$)	T_{edge} (eV)	Q (MW)	\bar{n} (10^{13} cm $^{-3}$)	\bar{T} (eV)	$\Delta_{\text{S.O.}}$ (cm)	Δ (cm)	R	Γ_p (10^{21} s $^{-1}$)	f (%)	
1. Base	5.0	140	48	1.15	24.5	5.6	3.3	0.80	4.7	63	
2. $\chi = 3 \times 10^4$ cm 2 /s	5.0	116	49	0.80	26.5	8.1	5.4	0.87	2.8	52	
3. $D = 3 \times 10^4$ cm 2 /s	5.0	103	49	1.60	21.0	7.0	4.1	0.71	8.6	52	
4. Low Q , low T_{edge}	4.6	100	30	1.30	23.0	5.3	3.0	0.76	5.8	61	
5. Low Q , moderate T_{edge}	4.0	112	30	1.10	24.0	5.3	3.3	0.80	4.5	62	
6. Lower temperature for recycling cutoff	4.0	112	30	0.92	21.2	7.6	5.6	0.30	4.2	48	
7. High neutral recycling on front of limiter	4.0	116	30	1.20	23.5	5.5	3.3	0.78	5.2	62	
8. Divertor case	4.5	165	30	2.7	43	5.7	-	0.86	4.4	17	

This condition results in a slightly lower recycling than case 1 because of the reduced neutral ionization probability. The lower recycling in case 3 coupled with the higher average density at the throat results in the highest pumping rate of any of the cases shown in Table 1. Rather than specify the fraction of the S.O. that flows below the limiter, the location of the leading edge is determined here by the criterion that the heat flux has fallen to 200 W/cm². The fraction of plasma flowing out of the S.O. that goes below the limiter is ≈ 10 to 20%. This fraction tends to increase as R decreases.

Cases 4-7 in Table 1 use edge densities and temperatures that result in integrated heat fluxes Q of 30 MW. These cases generally have a smaller portion of the S.O. impinging on the front surface of the limiter, but the parameters for the part of the S.O. flowing behind the limiter are similar to those of cases 1-3. The largest pumping rate found in cases 4-7 is for the low edge temperature example (case 4), which has the lowest recycling. The lower input for the edge temperature has the consequence of a lower average throat temperature (and even lower temperatures near the neutralizer plate) than the other cases, which is responsible for the small recycling value. The last two examples in Table 1 indicate little effect on the neutral pumping rates from changes in the assumptions about the recycling profile used in the radial profile model.

In general, the cases in Table 1 with the lowest recycling have the highest neutral pumping rates. Also it is seen that variations of the assumptions used in the model indicate factors of uncertainty on the order of 2. The neutral pumping rate required for a next step ignition device with 250 MW of fusion power and a 5% helium density ratio is $\approx 2 \times 10^{21}$ s⁻¹ (assuming helium transport (neutral and plasma) is equivalent to that of hydrogen). The neutral pumping rates shown in Table 1 indicate that adequate neutral particle removal rates for the exhaust requirements are possible for the pump-limiter configuration with $S_{\text{eff}} = 2.2 \times 10^5$ L/s.

All results to this point have been calculated using the same pump speed. Figure 4 shows the variation of the neutral pumping rate with different pump speeds. These results are for the same input conditions as case 5 in Table 1. The increase in neutral pumping rates with higher pumping speeds is primarily due to two effects: (1) lower neutral recycling and (2) a larger fraction of the plasma that flows into the throat being pumped as neutrals (pumping fraction) instead of escaping back toward the main plasma. The plasma flow into the throat for the 4.5×10^5 L/s example is approximately twice that of the 6×10^4 L/s example, and

this difference is related to the higher neutral recycling for the latter case. Also, the pumping fraction of the plasma flow into the throat is 2.5 times higher for the 4.5×10^5 L/s case compared to the 6×10^4 L/s case. The combination of the two effects results in a pumping rate that is approximately 5 times higher for the 4.5×10^5 L/s case. A divertor case (case 8) is also listed in Table 1. This case is for a heat flux of 30 MW, $S_{\text{eff}} = 2.1 \times 10^5$ L/sec and also uses $\chi = D = 10^4$ cm²/sec. The divertor channel geometry (Fig. 1) is more open for neutral penetration toward the main plasma than the limiter-channel geometry. As a result, a larger fraction of the neutral flux leaving the divertor channel exits as neutral escaping toward the main plasma rather than as pumped neutrals. In this case, only about one-fifth of the neutrals leaving the divertor channel are pumped, compared to corresponding fractions of more than one-half for the pump-limiter cases in Table 1.

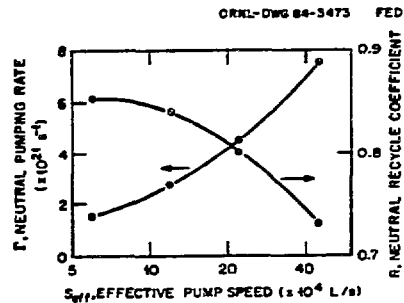


Fig. 4. Neutral pumping rate and neutral recycling vs. effective pump speed for a limiter case.

Variation of the neutral pumping rate vs. S_{eff} for the conditions used in the preceding case is shown in Fig. 5. The increase in neutral pumping rates with larger S_{eff} is caused by a larger fraction (F) of the plasma flow being pumped into the divertor channel. Unlike the pump limiter cases, the recycling is insensitive to changes in S_{eff} , and the total plasma flow rate into the divertor only changes slightly with S_{eff} . The lack of sensitivity of R to changes in S_{eff} is due to the small percentage of neutrals leaving the divertor channel as pumped neutrals. Also, it is evident that the neutral pumping rates for divertors are comparable to those of pump-limiters. Although the divertor case has more plasma flowing into the divertor channel than the limiter case, the smaller percentage of it that is pumped tends to even out the net pumping rate. To satisfy

the exhaust requirement of a particle removal rate $> 2 \times 10^{21} \text{ s}^{-1}$ from Fig. 5, it is seen that $S_{\text{eff}} > 10^5 \text{ L/s}$.

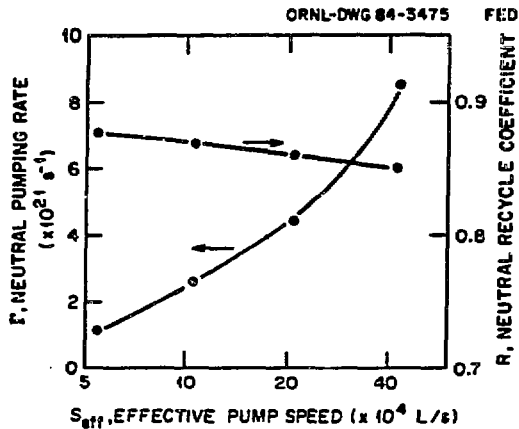


Fig. 5. Neutral pumping rate and neutral recycling vs. effective pump speed for a divertor case.

IV. SUMMARY

Investigation of the scrape-off region requires modeling the plasma transport along and across field lines and including the associated effects of neutral recycling. The method used in this work involves the use of separate models for each of these aspects that are coupled through an iteration procedure that checks the assumptions of one component with the output from another, and requires only minimal numerical effort. The method was applied here to the study of neutral pumping rates in the pump limiter and divertor options for a next step ignition experiment. It was found that high neutral recycling in the vicinity of the neutralizer plate has important ramifications on the evaluation of pumping rates for both the pump-limiter and divertor. In both cases, the plasma flow into the channel surrounding the neutralizer plate is greatly reduced by the neutral recycling. The fraction of this flow that is pumped can be large ($> 50\%$) but in general it is dependent on the particular geometry and plasma conditions. It was found that pumping speeds $> 10^5 \text{ L/s}$ are adequate for the exhaust requirements in the pump-limiter and the divertor cases.

REFERENCES

1. H.C. Howe, "Physics Considerations for the FED Limiter," ORNL/TM-7803, Oak Ridge Natl. Lab., 1981.

2. M. Ulrickson, "Optimum Shapes for Pump Limiters," PPPL-1901, Princeton Plasma Physics Lab., Princeton, N.J., 1982.
3. M. Ulrickson, "Particle and Energy Transport in the Plasma Scrape-off Zone and its Impact on Limiter Design," PPPL-1987, Princeton Plasma Physics Lab., Princeton, N.J., 1983.
4. J.M. Ogden et al., IEEE Trans. Plasma Sci. PS-9, 274 (1981).
5. A.T. Mense and G.A. Emmert, Nucl. Fusion 19, 361 (1979).
6. M. Petravac, D. Heifetz, and D. Post, J. Nuc. Mater. 111 & 112, 294 (1982).
7. M. Petravac et al., Phys. Rev. Lett. 48, 326 (1982).
8. P.T. Harbour and J.G. Morgan, "Models and Codes for the Plasma Edge Region," CLM-R-234, Culham Lab., Abingdon, England, 1982.
9. M. Shimada and JAERI Team, J. Nucl. Mater. 121, 126 (1984).
10. W. Schneider et al., J. Nucl. Mater. 121, 178 (1984).
11. M.F.A. Harrison, P.J. Harbour, and E.S. Hotson, Nucl. Technol./Fusion 3, 432 (1982).
12. E. Cupini et al., "Monte Carlo Studies of Helium Pumping and Sputtering in the INTOR Divertor," Commission of the European Communities Directorate General XII-Fusion Programme, Brussels, 1984.
13. J. Galambos and M. Peng, "Two Point Model for Divertor Transport," ORNL/FEDC-83/14, Fusion Engineering Design Center, Oak Ridge, Natl. Lab., 1984.
14. J. Galambos and M. Peng, J. Nucl. Mater. 121, 205 (1984).
15. J. Galambos, M. Peng, D. Heifetz, "Coupled Plasma Neutral Transport Model for the Scrape-off Region", ORNL/FEDC/84/6, Fusion Eng. Design Center, Oak Ridge Natl. Lab., 1984.
16. D. Heifetz et al., J. Comput. Phys. 46, 309 (1982).